

The Neglected Tails of Vision-Language Models

Shubham Parashar^{*1} Zhiqiu Lin^{*2} Tian Liu^{*1} Xiangjue Dong¹
 Yanan Li³ Deva Ramanan² James Caverlee¹ Shu Kong^{14†}

¹Texas A&M University ²Carnegie Mellon University ³Zhejiang Lab ⁴University of Macau

Abstract

Vision-language models (VLMs) excel in zero-shot recognition but exhibit drastically imbalanced performance across visual concepts. For example, CLIP, despite an impressive mean zero-shot accuracy on ImageNet (72.7%), yields <10% on ten concepts (e.g., gyromitra and night snake), presumably because these concepts are under-represented in VLMs’ imbalanced pretraining data. Yet, assessing this imbalance is challenging as it is non-trivial to calculate the frequency of specific concepts within VLMs’ large-scale pretraining data. Our work makes the first attempt to measure the concept frequency by analyzing pretraining texts. We use off-the-shelf language models to help count relevant texts that contain synonyms of the given concepts and resolve linguistic ambiguity. We confirm that popular VLM datasets like LAION indeed exhibit long-tailed concept distributions, which strongly correlate with per-class accuracies. Further, contemporary multimodal systems, e.g., visual chatbots and text-to-image generators, also struggle with the rare concepts identified by our method. To mitigate VLMs’ imbalanced performance in zero-shot recognition, we propose REtrieval-Augmented Learning (REAL). First, instead of prompting VLMs using the original class names, REAL uses their most frequent synonyms found in VLMs’ pretraining texts. This already outperforms human-engineered and LLM-generated prompts over nine benchmark datasets, likely because VLMs have seen more images associated with the frequently used synonyms. Second, REAL uses all the concept synonyms to retrieve a small, class-balanced set of pretraining data to train a robust classifier. REAL surpasses the recent retrieval-augmented solution REACT, using 400× less storage and 10,000× less training time!

1. Introduction

Vision-language models (VLMs) such as CLIP [33] play a pivotal role in mainstream multimodal applications, including visual chatbots [21, 29] and text-to-image generation [3, 34]. Their efficacy largely derives from their large-

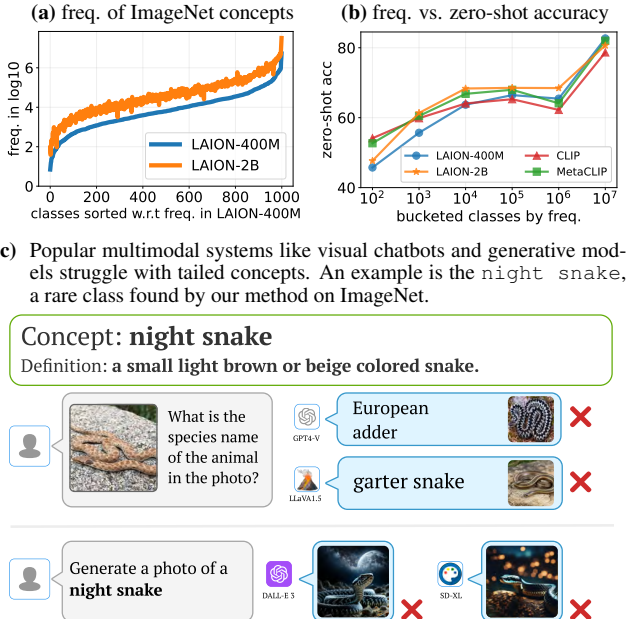


Figure 1. **Vision-language models (VLMs) inherit long tails from their pretraining data.** (a) VLMs’ pretraining datasets, such as LAION-400M [35] and LAION-2B [36], exhibit long-tailed distributions for visual concepts defined in downstream tasks like ImageNet [9]. We sort the 1K ImageNet classes according to their frequency in LAION-400M calculated with our concept frequency estimation method (cf. Fig. 2). (b) For zero-shot recognition, OpenCLIP models [14] trained on LAION-400M and LAION-2B respectively yield per-class accuracies that strongly correlate with the long-tailed concept frequencies (binned on a log-scale). Interestingly, other VLMs such as CLIP [33] and MetaCLIP [47] (trained on private data) also show similar imbalanced performances, likely because their web-scraped pretraining datasets follow similar long-tailed distributions of the real world. (c) Our method helps identify rare concepts, such as the **night snake**, which is one of the most tailed ImageNet concepts. We show that state-of-the-art multimodal systems, including GPT4-V [48], LLaVA [21], DALL-E 3 [39], and SD-XL [2], all fail to recognize or generate it. The supplement contains more examples.

scale image-text pretraining datasets like LAION [35, 36] that encompass broad visual concepts.

Imbalanced performance of VLMs. Despite their impressive visual understanding capabilities, VLMs exhibit an imbalanced performance in downstream tasks. For exam-

^{*}Co-first authors; [†]corresponding author. Project page at [link](#).

ple, in the established zero-shot recognition task where no training examples are available, CLIP [33] yields a high mean accuracy (72.7%) across 1K semantic classes on ImageNet [19] but only <10% accuracy on ten classes (e.g., gyromitra and night snake) (Fig. 1b). This motivates us to delve into the imbalanced performance of VLMs (e.g., CLIP [33] and OpenCLIP [14]) through the lens of zero-shot image recognition.

Why do VLMs exhibit imbalanced performance? A plausible reason is their inherent bias [50], which originates from the imbalanced distribution of visual concepts in their pretraining data. However, to date, the literature has not established a clear link between VLMs’ imbalanced performance and the concept distribution in their training datasets, presumably because estimating *concept frequency* in such large-scale, multimodal pretraining data is non-trivial.

Concept frequency estimation. Estimating class frequency in a typical classification dataset is straightforward, where counting class occurrences in annotated labels is sufficient. But estimating concept frequency in VLMs’ pretraining datasets is non-trivial, as they contain free-form texts with significant *lexical variation*, e.g., a sneaker can also be referred to as a running shoe or a trainer. To address this, we leverage off-the-shelf large language models (LLMs). Fig. 2 illustrates our approach, which begins by asking an LLM (such as ChatGPT [29]) to enumerate all synonyms for a specific concept. We then use string matching to find all pretraining texts that contain the concept or its synonyms. However, due to *linguistic ambiguity*, the initially retrieved texts can include unrelated phrases, such as “tiger shark in water” for the target concept tiger (a mammal). We again use an LLM to filter out irrelevant texts to the target concept and only count relevant ones for its frequency measure. Our simple method for calculating concept frequency allows us to, for the first time, unveil three key insights: (1) it exposes long-tailed concept distributions in VLMs’ pretraining data (Fig. 1a); (2) it establishes a correlation between the long-tailed distribution and VLMs’ imbalanced performance (Fig. 1b); and (3) it sheds light on why the cutting-edge foundational models (e.g., GPT4-Vision in Fig. 1c) fail to recognize images featuring rare concepts. Importantly, our analysis provides insights that facilitate the exploration of approaches (explained below) to enhance VLMs in downstream tasks such as zero-shot image recognition.

Improving VLMs’ zero-shot performance. Motivated by our analysis, we present **REtrieval-Augmented Learning (REAL)** to address the biased predictions of VLMs, thereby greatly improving VLMs’ zero-shot recognition performance. REAL has two variants. First, observing that some synonyms appear more frequently in VLM’s pretraining data than the original concept names, we propose **REAL-Prompt**. It replaces the original concept names

with their *most frequent synonyms* for zero-shot recognition. For example, we substitute cash machine with ATM, as the latter appears ten times more frequent in LAION (Fig. 3). This simple change already surpasses previous methods that use either human-engineered prompts [33] or LLM-generated ones [26, 32] (cf. Table 1). We attribute its success to VLMs’ greater exposure to these more frequent synonyms, which improve their accuracy in recognizing related images. Second, inspired by retrieval-augmented strategies [10, 17, 18, 22, 42], we introduce **REAL-Linear**, which reuses relevant pretraining data to better adapt VLMs for zero-shot recognition without using data from downstream tasks. The key idea is to retrieve a small, class-balanced set of images from pretraining data to train a robust linear classifier [20]. In contrast to prior arts [22, 42] that perform costly *feature-based* retrieval by running VLMs to compute image or text features, our method implements *text-based* retrieval via string matching, achieving a significant boost in efficiency. As a result, our REAL resoundingly outperforms the recent retrieval-augmented solution, REACT [22], using 400 \times less storage and 10,000 \times less training time (cf. Table 1 and 3)!

Contributions. We summarize our major contributions.

- We propose a method for estimating the frequency of visual concepts within VLMs’ large-scale pretraining data. Our analysis, for the first time, exposes long-tailed concept distributions in popular datasets like LAION and reveals systematic failures of VLMs [2, 21, 39, 48] in handling rare concepts.
- To address the biased predictions of VLMs, we propose REAL to improve their zero-shot performance without using data from downstream tasks. REAL establishes a new state-of-the-art in zero-shot recognition through its efficient prompting and retrieval-augmented training strategies.

2. Related Works

Biases in foundation VLMs. Pretrained on expansive multimodal datasets [4, 7, 43], VLMs often exhibit biases related to gender, race, and geography [25], leading to imbalanced predictions in downstream applications [1, 27]. Such biases likely stem from data imbalances in their pretraining set [50]. Recent studies [37, 45, 50] seek to mitigate imbalanced predictions of VLMs by training on additional data from downstream tasks. Despite these efforts, there has been a lack of analysis of the imbalances in the pretraining data itself. Our study presents the first direct analysis of VLMs’ pretraining data, uncovering a long-tailed distribution of concepts and its strong correlation with the imbalanced performance of VLMs. Our analysis tool can also help researchers identify rare, inadequately learned concepts in VLMs, reducing the risk of biased predictions.

Prompting VLMs for zero-shot recognition. VLMs

demonstrate remarkable capabilities in zero-shot recognition tasks, where only the names of target concepts are provided without corresponding training images. CLIP [33] shows that ensembling concept names with human-engineered prompt templates, such as “a photo of a {class}” and “a demonstration of a {class}”, often enhances zero-shot recognition. Approaches like DCLIP [26] and CuPL [32] employ LLMs (e.g., GPT-3) to create class-specific prompts with visual descriptions, for example, “a tiger, which has sharp claws”. While most works focus on refining prompt templates [23, 38, 49], they use the provided class names as is. A recent work [30] suggests that prompting with common English names instead of Latin scientific names improves zero-shot recognition of fine-grained species. Differently, our method proposes to replace the original class names with their most common synonyms found in the pretraining dataset. This simple change already outperforms existing methods that strive to improve prompt templates. Moreover, our approach can be integrated with existing methods to further improve their zero-shot recognition performance.

Retrieval-augmented strategy. The natural language processing (NLP) literature introduces this strategy to address challenging tasks such as knowledge-based question-answering [10, 17]. For example, in order to produce a better answer given a question, this strategy retrieves relevant facts from an external knowledge base (e.g., the Internet or pretraining dataset) to ground LLMs on the most accurate, up-to-date information. To improve zero-shot visual recognition, recent works [18, 22, 42] propose to fine-tune VLMs on relevant images retrieved from VLMs’ pre-training datasets for better accuracy. While solutions such as REACT [22] are effective across diverse target domains, they require significant computing resources, such as hundreds of GPU hours and intensive memory usage for large-batch contrastive training. In contrast to these works, we propose a lightweight solution that retrieves data by fast string matching of concept synonyms in pretraining texts, bypassing the heavy computation of VLM features. Moreover, we learn a robust, parameter-efficient linear classifier atop the frozen VLM, enhancing training efficiency. Our solution not only outperforms existing computationally intensive approaches, but also offers an opportunity for research on retrieval-augmented strategy with modest compute.

3. The Long-Tailed Concept Distribution

This section describes our approach for estimating concept frequency in VLM’s pretraining data, followed by a discussion of our key findings.

3.1. Concept Frequency Estimation

The foremost challenge in estimating concept frequency is the sheer size of a VLM’s pretraining dataset. For ex-

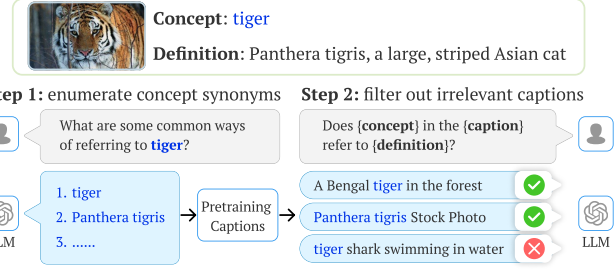


Figure 2. **Using large language models (LLMs) to estimate concept frequency in a VLM’s pretraining dataset.** We conduct the frequency estimation using publicly available LAION [35] datasets. First, since a visual concept can be expressed in various ways, we ask an LLM (e.g., ChatGPT [29]) to enumerate all its synonyms to search for all relevant pretraining texts. For example, for *tiger*, we retrieve all captions that contain not only “*tiger*” but also its synonyms such as “*Panthera tigris*”, using efficient string matching. Second, we filter out irrelevant captions that do not refer to the target concept by its definition. For example, although “*tiger shark swimming in water*” contains “*tiger*”, it actually refers to a type of shark, not the animal *tiger* as defined by “*Panthera tigris, a large, striped Asian cat*”. We conduct the filtering process by querying an LLM (cf. Section 3).

ample, the popular open-source LAION-400M [36] dataset (used for training OpenCLIP [14]) takes \sim 10TB of physical space. We instead estimate concept frequency directly from pretraining texts, bypassing the need for pretraining images. This enables us to download just the text metadata, requiring only 60GB space for LAION-400M. Our method consists of the following two steps (cf. Fig. 2).

Step 1: Deriving synonyms for concepts of interest. A well-known issue in NLP is *lexical variation*, meaning that a concept can be expressed in multiple ways. For example, “*sneaker*” can be referred to as “*running shoes*” or “*athletic footwear*”, and “*tiger*” may also be called “*Panthera tigris*”. To account for the lexical variation in concept frequency estimation, we first derive a list of synonyms¹ for a given visual concept. To do so, we turn to an off-the-shelf LLM (e.g., ChatGPT [29]), by asking a simple question “*What are some common ways of referring to {concept}?*”. With all the synonyms, we retrieve relevant pretraining texts using string matching. The string matching process is quite efficient — it takes only 5 hours to retrieve 400M pretraining texts from LAION-2B containing ImageNet’s 1K concepts.

Step 2: Filtering out irrelevant pretraining texts. Using simple string matching to retrieve pretraining texts may be inaccurate due to *linguistic ambiguities*. For instance, the concept “*tiger*”, defined as “*Panthera tigris, a large, striped Asian cat*”, might appear in unrelated contexts in

¹For simplicity, we use the term “synonyms” in a broader sense to encompass all forms of lexical variation, including but not limited to traditional synonyms, idiomatic expressions, and different phrasings that convey the same or similar meanings.

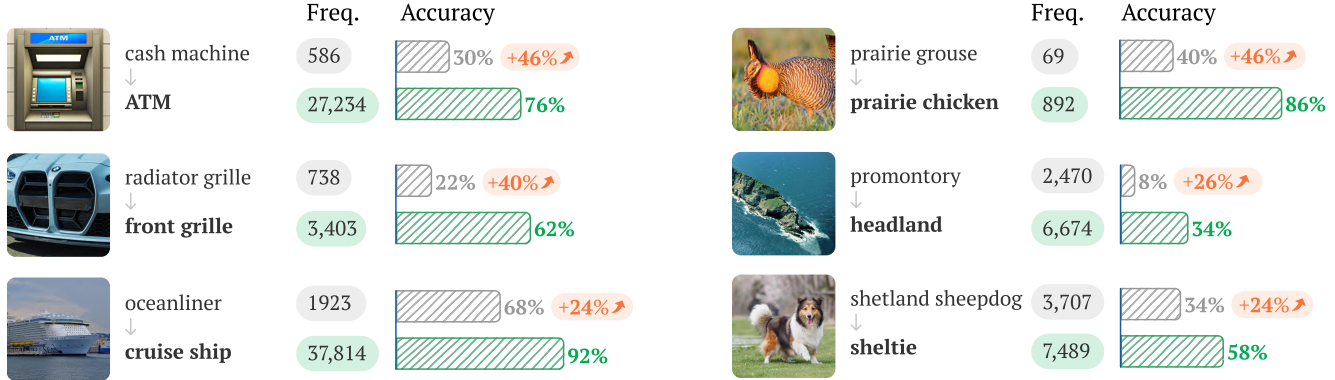


Figure 3. **Demonstration of REAL-Prompt**, which replaces the given concept names (e.g., “cash machine”) with their most frequent synonyms (e.g., “ATM”) in the prompt template, e.g., “*a photo of {concept}*”. REAL-Prompt uses an LLM (ChatGPT) to obtain synonyms for a given concept, followed by string matching to identify the most frequently occurring ones in pretraining texts. We demonstrate REAL-Prompt on some ImageNet concepts with their most frequent synonyms, frequencies (in LAION-400M), and per-class accuracies. The simple change in prompts significantly improves zero-shot recognition. We detail the procedure for REAL-Prompt in Sec. 4.1 and compare against prior works in Table 1.

the retrieved captions such as “*tiger shark swimming in water*” and “*Tiger Woods, a famous golf player*”; in these texts, the “tiger” actually refers to a shark species and a celebrity, respectively. To tackle these ambiguities at an affordable cost, we utilize the state-of-the-art open-source LLM Llama-2 [40]. For each retrieved text, we ask:

Does {concept} in the {caption}
refer to {definition}?

In real-world applications, concepts are typically defined in the labeling policies of downstream tasks. In this work, to align with standard benchmarks, we adopt definitions from Elevater [19]. Finally, captions identified as irrelevant to the target concept by the LLM are excluded from retrieved data.

3.2. Discussions and Remarks

Human-in-the-loop validation. As VLMs’ pretraining data does not contain ground-truth concept labels, we also perform manual validation. To do so, we first construct a small validation set by downloading a balanced set of pre-training data (32 image-text pairs per concept). Then, for each concept, we tune the concept definitions for Llama-2 till reaching $>85\%$ retrieval precision on the validation set. In particular, since [19] releases multiple definitions per concept, we select the best ones that lead to the highest precision over the validation set. For example, the class *samoyed* in ImageNet refers to a dog breed; we find the definition “*a breed of large white herding dog with a thick coat, native to the Ural Mountains*” to be more precise than others, e.g., “*a member of a people inhabiting northwestern Siberia*”. To facilitate future research, we will open-source our code for LLM-based analysis and release all concept synonyms and filtered captions.

The prevalent long tails in VLMs. Our analysis reveals a notable long-tailed distribution of visual concepts (from

standard benchmarks like ImageNet [9]) within widely-used pretraining datasets like LAION-400M and LAION-2B (cf. Fig. 1a). Additionally, we plot per-class zero-shot accuracies of OpenCLIP models (pretrained on LAION), establishing a strong correlation between the long-tailed distribution of concepts and the imbalanced performance of VLMs (cf. Fig. 1b). We also plot the per-class accuracies of CLIP [33] and MetaCLIP [47], which are trained on private datasets. Interestingly, they show similar imbalanced performances across ImageNet’s concepts. We observe the same long-tailed concept frequencies and imbalanced per-class accuracies across eight more benchmarks (cf. Table 7), e.g., Flowers [28] and Pets [31]. Notably, our method can find rare (tailed) concepts that challenge downstream models including the state-of-the-art GPT-4Vision [29] and DALL-E 3 [39] (cf. Fig. 8 and 9). In sum, our analysis shows the prevalent long-tail issues in VLMs.

Are long tails inevitable in large-scale data curation? Despite the imbalanced performance of CLIP [33] and MetaCLIP [47], their pretraining datasets are actually created using a “balanced” sampling strategy. Specifically, they define 500K word phrases as web search queries to collect approximately equal numbers of image-text samples for each. However, our analysis indicates that these datasets (which are not fully disclosed to the public) might not be as balanced as intended. We identify key insights into the observed imbalances by examining [47]’s query statistics:

- **Internet data are naturally long-tailed:** Despite balanced sampling in [47], the resulting distribution is still long-tailed. For example, while each search query is capped at 20K images, the average is around $\sim 1.2K$ images per query. In fact, we find that over half of the queries, such as “tailed frog” (a frog), “gyromitra” (a fungus), and “poke bonnet” (a

traditional hat), have fewer than 50 samples, likely because these concepts are rare on the web.

- **Limitations of query-based balancing:** Balancing per query does not guarantee a balanced distribution of concepts. For example, [47] inadvertently include overlapping queries such as “sneaker” and “running shoes”, which can lead to the overrepresentation of certain concepts. Moreover, samples retrieved for a single query often contain other concepts. For instance, samples featuring “keyboard” may also frequently include “mouse” and “computer”.

As curating a perfectly balanced pretraining dataset is challenging, we recommend that researchers acknowledge the presence of long tails and prioritize addressing VLM’s imbalanced performances in downstream applications.

4. Retrieval-Augmented Learning

To address the biased performance of VLMs in zero-shot recognition, we propose **RE**trieval-Augmented **L**earning (REAL), which improves performance without using any data from downstream tasks by retrieving pretraining data relevant to the target concepts. REAL has two variants: REAL-Prompt and REAL-Linear. REAL-Prompt is a novel prompting strategy that replaces the original concept name with its most frequent synonym found in the pretraining texts. REAL-Linear retrieves images relevant to the concepts from the pretraining data to form a class-balanced dataset and use this set to learn a robust linear classifier. Below we elaborate on these two methods.

4.1. REAL-Prompt for Zero-Shot Prompting

In our analysis, we discover that some synonyms for a concept might be more frequent in pretraining texts than the concept itself. Therefore, we propose using the most frequent synonym of a concept to construct prompts. Specifically, we utilize an LLM (ChatGPT [29]) to enumerate all synonyms for each concept. Next, we count their individual frequencies in the pretraining texts by string matching. We use the most frequent synonym of each concept in the prompt to construct an off-the-shelf classifier W_{zs} for zero-shot recognition following CLIP [33]. This simple change leads to notably better zero-shot accuracy than using the original concept names (cf. Fig. 3) released by [33], which are hand-crafted over one year. As shown in Table 1, our approach also outperforms recent LLM-based prompting methods that use additional visual descriptors along with the given concept names (e.g., DCLIP [26] and CuPL [32]).

Synonym filtering using OpenCLIP’s text encoder. ChatGPT sometimes generate noisy synonyms. For example, for “tiger”, it lists “big cat” as a synonym, which could be easily confused with the ImageNet class “tabby cat”. To address this, we use OpenCLIP’s text encoder to

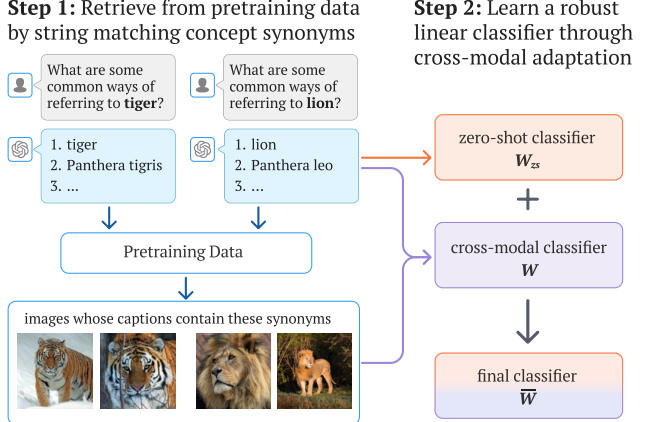


Figure 4. **Flowchart of REAL-Linear.** First, it uses all synonyms of the given concepts to retrieve a class-balanced subset of pretraining images (e.g., 500 images per class from the dataset LAION-400M). Next, it learns a linear classifier W atop the frozen VLM using cross-modal adaptation [20], and then ensembles it with the off-the-shelf classifier W_{zs} , whose weights are text prompt embeddings based on the most frequent synonyms.

filter out synonyms that might be confused with other downstream concepts. We retain only those synonyms that have the highest cosine similarity scores with their original class names. This filtering step is fully automated, ensuring a fair comparison with [26, 32] that perform LLM-based prompting without human input. We show that this step is crucial to REAL-Prompt’s performance in Table 15.

4.2. REAL-Linear for Linear Classifier Training

To further improve performance, REAL-Linear finetunes on images retrieved from pretraining data that are relevant to target concepts, as illustrated in Fig. 4.

Step 1: Retrieving data using concept synonyms. For each concept, we retrieve pretraining data (LAION) whose textual captions contain any concept synonyms from REAL-Prompt. Then, we sort the retrieved data by the cosine similarity between their captions and the averaged text features (generated by OpenCLIP’s text encoder using all concept synonyms). We select an equal number of the top-ranked images per concept (e.g., 500) to ensure a class-balanced dataset.

Step 2: Training a robust linear classifier. To address the potential domain gap between the pretraining data and the downstream task, we construct a robust linear classifier W using cross-modal adaptation [20]. Concretely, we learn a linear classifier W atop VLM’s embeddings of the retrieved images and concept names, and then ensemble it with the zero-shot classifier W_{zs} (i.e., REAL-Prompt): $\bar{W} = W + W_{zs}$.

REAL-Linear’s exceptional efficiency. REAL-Linear is significantly more efficient than the state-of-the-art RE-

Table 1. **REAL outperforms existing methods on standard zero-shot recognition datasets.** Within the zero-shot prompting paradigm, our REAL-Prompt that prompts with the *most frequent synonyms* of visual concepts (using OpenAI’s templates [33]) outperforms existing prompting approaches that adopt the original concept names, such as DCLIP [26] and CuPL [32]. Within the retrieval-augmented learning paradigm (without using any data from downstream tasks), our REAL-Linear retrieves a class-balanced subset of pretraining data (500 examples per concept from LAION-400M), learns a linear classifier ensembled with the zero-shot classifier used by REAL-Prompt. REAL-Linear rivals the recent method REACT [22] (which retrieves 10K examples per concept), and importantly, uses 5% of REACT’s retrieved images and 1% of its compute as detailed in Table 3. We highlight the **best accuracy** in bold and underline the second best numbers.

	Method	ImageNet	Flowers	Cars	Aircraft	Pets	Food	DTD	EuroSAT	Avg
Zero-Shot Prompting	prompt template “{concept}”	60.7	63.8	78.1	12.6	83.3	80.1	48.8	28.6	57.0
	“a photo of {concept}”	62.5	66.5	77.2	15.8	84.0	80.3	52.8	36.6	59.5
	OpenAI templates [33]	62.9	<u>68.0</u>	79.2	16.7	86.7	<u>80.9</u>	54.5	<u>51.5</u>	62.6
	DCLIP [26]	62.1	—	—	—	84.6	80.1	51.9	36.8	—
	CuPL [32]	63.7	65.8	<u>80.0</u>	<u>17.8</u>	<u>87.4</u>	79.5	<u>59.1</u>	—	—
	REAL-Prompt	<u>63.6</u>	76.6	82.7	18.0	88.8	81.0	59.9	57.5	66.0
Retrieval Augmented	REACT (10K) [22]	—	—	—	—	—	—	—	—	—
	Locked-Text	<u>65.7</u>	<u>73.1</u>	88.5	24.5	89.2	81.8	49.8	<u>51.1</u>	<u>65.5</u>
	Gated-Image	64.2	72.3	<u>88.1</u>	<u>24.8</u>	<u>89.5</u>	83.0	<u>51.4</u>	45.4	64.8
	REAL-Linear (500)	65.9	78.8	84.4	29.6	89.5	81.4	61.5	51.5	67.8

ACT [22] and can be done using only academic-scale compute resources. Unlike REACT, which requires running VLMs to extract features from all pretraining images and texts, REAL-Linear processes only pretraining texts via string matching. As a result, it can process all LAION-400M captions in one hour, whereas REACT needs 250 GPU hours just for feature extraction. In addition, REACT’s contrastive training demands extensive resources for better performance, e.g., large batch sizes (4,096) and lengthy training (up to 256 GPU hours on 16 V100 GPUs). In contrast, our linear-probing approach trains in minutes on a modest (12GB) GPU. Table 3 compares the efficiency between REACT and REAL.

5. Experimental Results

We assess REAL’s performance in zero-shot recognition tasks, comparing it against prior works on standard benchmarks. We also ablate design choices in REAL that contribute to its performance. Moreover, we show that integrating REAL with existing methods leads to improved results. Lastly, we explore an application of REAL-Prompt in text-to-image models like DALL-E 3 and SD-XL, which improves image generation of rare concepts.

5.1. Experimental setup

Datasets and metric. We report mean per-class accuracy on standard classification benchmarks, including ImageNet [9], Flowers [28], Cars [16], Aircraft [24], Pets [31], Food [5], DTD [8], EuroSAT [11], and CUB [41]. Moreover, we use variants of ImageNet to study the robustness of our methods, including ImageNet-V2 [15], ImageNet-Adversarial [13], ImageNet-Rendition [12], and ImageNet-Sketch [44]. Table 6 lists their detailed descriptions.

Table 2. **REAL boosts both head and tail performance.** We show that REAL-Prompt and REAL-Linear (500 retrieved examples per concept) achieve consistent improvement across all classes over the baseline using OpenAI templates [33]. On each dataset, we define the tail as the 20% least frequent classes and the rest as the head, and report the averaged per-class accuracy over nine standard zero-shot recognition datasets (including CUB [41]). We report detailed improvements on each dataset in Table 8.

	Method	ImageNet		Avg of 9 datasets	
		Head	Tail	Head	Tail
LAION 400M	OpenAI templates	64.8	55.2	65.7	52.5
	REAL-Prompt	<u>65.4</u> ^{+0.6}	<u>56.2</u> ^{+1.0}	<u>67.8</u> ^{+2.1}	<u>56.9</u> ^{+4.4}
	REAL-Linear	<u>67.8</u> ^{+3.0}	<u>58.9</u> ^{+3.7}	<u>72.5</u> ^{+6.8}	<u>56.0</u> ^{+3.5}
LAION 2B	OpenAI templates	<u>68.0</u>	61.0	68.6	58.4
	REAL-Prompt	<u>68.2</u> ^{+0.2}	<u>61.6</u> ^{+0.6}	<u>69.8</u> ^{+1.2}	<u>61.8</u> ^{+3.4}
	REAL-Linear	<u>69.8</u> ^{+1.8}	<u>64.8</u> ^{+3.8}	<u>76.2</u> ^{+7.6}	<u>63.6</u> ^{+5.2}

Compared methods. We compare against state-of-the-art zero-shot recognition methods for VLMs. We report various prompting strategies that directly use the given concept names, including prompt templates such as “{concept}”, “a photo of {concept}”, and OpenAI’s hand-engineered templates [33]. We also compare with LLM-based prompting methods, DCLIP [26] and CuPL [32], which uses GPT to generate descriptions for constructing prompts. Finally, we compare our method with the retrieval-augmented method REACT [22]. We report two variants of REACT: Locked-Text and Gated-Image.

Implementation details. In this work, we adopt a series of OpenCLIP VLMs [6, 14], which are publicly available along with their two pretraining datasets, namely LAION-400M [35] and LAION-2B [36]. We report the performance of OpenCLIP ViT-B/32 architecture in the main paper and show that REAL generalizes to other architectures in Ta-

ble 13. For our method REAL-Linear that learns a linear classifier, we simply use the hyperparameters provided by prior work [20, 46]. We use a single GeForce RTX 2080 Ti (12GB) to train all the models and allocate 50GB of storage to host retrieved data for all the nine benchmark datasets.

5.2. Results

Using frequent synonyms improves zero-shot recognition. Table 1 (top half) compares REAL-Prompt (based on OpenAI’s prompt templates) against other prompting-based methods like DCLIP [26] and CuPL [32], which use GPT to generate visual descriptions. REAL-Prompt significantly outperforms them simply by replacing the original concept names with their most frequent synonyms. This underscores the importance of re-considering concept names in prompting; using the frequently used synonyms improves the recognition of related images.

REAL-Linear achieves the state-of-the-art. Table 1 (bottom half) compares our REAL-Linear against the recent retrieval-augmented method REACT [22]. REAL-Linear achieves $\sim 3\%$ higher accuracy averaged across eight benchmarks than REACT, while using only 500 retrieved images per concept compared to REACT’s 10K. Importantly, REAL-Linear is significantly more efficient (cf. Table 3): it requires $\sim 1\%$ of REACT’s computes, making it more accessible to the research community.

REAL benefits both head and tail classes. Table 2 shows that REAL boosts performance for both tail (least frequent 20%) and head (the rest 80%) classes on ImageNet and all nine datasets. For more specific improvements on each dataset, see Table 8.

REAL benefits existing zero-shot methods. Our methods can be readily applied with existing methods to further improve performance. Table 4 shows that REAL-Prompt’s most frequent synonyms can be applied on any prompt templates, including LLM-generated ones like DCLIP [26] and CuPL [32]. Likewise, REAL-Linear can be applied on top of REACT’s finetuned OpenCLIP models, which establishes a new state-of-the-art zero-shot performance as shown in Table 5.

Improving image synthesis using REAL-Prompt. Fig. 5 shows that, while state-of-the-art generative models such as DALL-E 3 [39] and SD-XL [2] may fail to generate correct images for some rare concepts (identified by frequency estimation on LAION-400M), replacing the rare concepts used in prompts with their most frequent synonyms (found by REAL-Prompt) can help generate more accurate images. More qualitative examples can be found in Fig. 10 and 11.

Ablation studies for REAL-Linear. Our experiments shed light on key design aspects of REAL-Linear, with major insights summarized below. Table 9 shows that using all concept synonyms, as opposed to just the original con-

Table 3. Compute cost comparison between REACT [22] and our REAL-Linear. We ablate resources required for each method on the ImageNet experiment. Clearly, REAL-Linear (retrieving 500 pretraining images per concept) uses much less compute than REACT, e.g., retrieving $1000\times$ less images, using $400\times$ less storage and $10,000\times$ less training time.

Stage	Resource	REACT [22]	REAL (500)	Relative Cost
Retrieval	retrieved examples	400M	0.5M	0.1%
	time	200 hrs	6 hrs	3%
	storage	10 TB	25 GB	0.25%
Learning	training images	10M	0.5M	5%
	time	256 hrs	2 mins	0.01%
	# of learned parameters	87M	0.5M	0.6%
	GPU memory	256 GB	3 GB	1%

cept names, can help retrieve more diverse pretraining data, improving the averaged accuracy by 4%. Table 11 demonstrates that learning the linear classifier with both text and image features using cross-modal WiSE-FT [20, 46] leads to a 6.4% increase compared to linear probing with only image features. Lastly, Table 12 shows that increasing the retrieval size from 100 to 500 per concept yields a modest accuracy improvement of 0.9%. Based on this, we adopt 500 as the standard retrieval size for our experiments.

5.3. Discussions

Broad impacts. Our work has positive societal impacts. Our concept frequency estimation method not only confirms the long-tailed distribution of concepts in VLMs’ pretraining data but also reveals a strong correlation with VLMs’ imbalanced or biased performances. By identifying concepts that VLMs insufficiently learn, we can implement targeted measures to prevent unfair or biased predictions related to these concepts.

Limitations and future work. We acknowledge several limitations in our methods. First, while we offer a method to estimate concept frequency, we cannot accurately evaluate its precision and recall due to the absence of ground-truth annotations of the pretraining data. Second, this approach relies only on textual captions and may overlook the broader concept coverage that images offer. Lastly, filtering ambiguous captions using off-the-shelf LLMs for each caption-concept pair is time-consuming. We expect the future work to address these limitations.

6. Conclusions

We explore the neglected long-tail issues existing in Vision-Language Models (VLMs). We present a novel method for estimating concept frequency in VLMs’ large-scale multimodal pretraining data. With our method, we reveal that concepts defined by downstream tasks (e.g., image classification) follow long-tailed distributions in the pretraining data. Importantly, for the first time, we establish

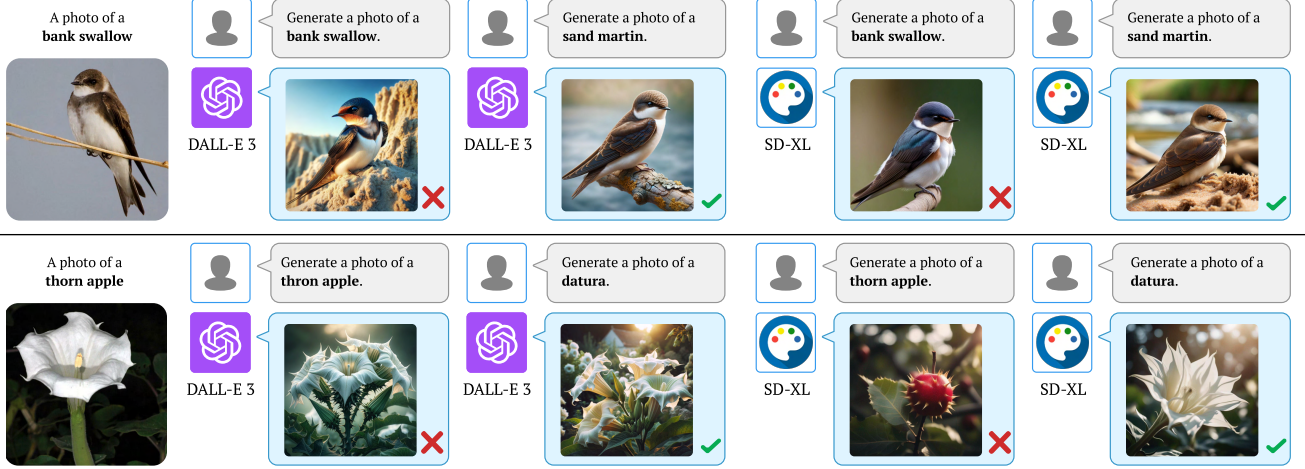


Figure 5. **Improving image generation using REAL-Prompt.** We show two rare concepts identified by our frequency estimation where DALL-E 3 and SD-XL struggle to generate accurate images: bank swallow (top, a bird from the CUB dataset) and thorn apple (bottom, a flower from the Flowers dataset). Using their original names, both DALLE 3 and SD-XL incorrectly render the bird’s colors. Additionally, DALLE 3 erroneously adds thorns to the flower, while SD-XL depicts an apple with literal thorns. Instead, using the most frequent synonyms (sand martin for bank swallow, datura for thorn apple) as found by REAL-Prompt results in both systems generating accurate images. See more examples in Fig. 10 and 11.

Table 4. **Improvements using REAL-Prompt with existing prompting methods.** Our REAL-Prompt can be combined with existing prompt templates including OpenAI’s hand-engineered templates and LLM-generated templates [33] like DCLIP [26] and CuPL [32]. On datasets such as Flowers, DTD, and EuroSAT, integrating REAL-Prompt results in an accuracy boost of 5~8%.

Prompting Method	ImageNet	Flowers	Cars	Aircraft	CUB	Pets	Food	DTD	EuroSAT
OpenAI templates [33]	62.9	68.0	79.2	16.7	63.8	86.7	80.9	54.5	51.5
+ REAL-Prompt	63.6 ^{+0.7}	76.6 ^{+8.6}	82.7 ^{+3.5}	18.0 ^{+1.3}	64.0 ^{+0.2}	88.8 ^{+2.1}	81.0 ^{+0.1}	59.9 ^{+5.4}	57.5 ^{+6.0}
DCLIP [26]	62.1	–	–	–	64.5	84.6	80.1	51.4	36.8
+ REAL-Prompt	62.9 ^{+0.8}	–	–	–	64.7 ^{+0.2}	88.1 ^{+3.5}	80.0 ^{-0.1}	55.5 ^{+4.1}	36.9 ^{+0.1}
CuPL [32]	63.7	65.8	80.0	17.8	–	87.4	79.5	59.1	–
+ REAL-Prompt	64.2 ^{+0.5}	72.3 ^{+6.5}	81.7 ^{+1.7}	18.3 ^{+0.5}	–	88.0 ^{+0.6}	79.5 ^{+0.0}	59.3 ^{+0.2}	–

Table 5. **Enhancing REACT’s robustness with REAL-Linear.** Our REAL-Linear (using 500 retrieved images per concept), when applied to REACT [22]’s finetuned OpenCLIP models (ViT-B/32 trained on LAION-400M), improves zero-shot accuracy across various challenging ImageNet variants. These variants, including ImageNet-V2 [15], ImageNet-Adversarial [13], ImageNet-Rendition [12], and ImageNet-Sketch [44], are specifically designed to assess model robustness against domain shifts.

Method	ImageNet	→ ImageNet Variants			
		V2 [15]	A [13]	R [12]	S [44]
OpenAI templates [33]	62.9	55.1	21.7	73.5	49.4
REAL-Linear	65.9 ^{+3.0}	57.3 ^{+2.2}	22.7 ^{+1.0}	73.9 ^{+0.4}	50.9 ^{+1.5}
REACT Locked-Text	65.7	57.2	20.3	77.6	54.8
+ REAL-Linear	67.7 ^{+2.0}	59.1 ^{+1.9}	21.3 ^{+1.0}	78.1 ^{+0.5}	55.9 ^{+1.1}
REACT Gated-Image	64.2	56.3	21.1	75.9	52.4
+ REAL-Linear	66.9 ^{+2.7}	59.1 ^{+2.8}	21.7 ^{+0.6}	76.8 ^{+0.9}	54.2 ^{+1.8}

the strong correlation between the long-tailed concept distributions and the imbalanced or biased performance (e.g., per-class accuracy in zero-shot recognition) of VLMs. Further, to mitigate VLMs’ imbalanced performance through the lens of zero-shot recognition, we propose retrieval-

augmented learning (REAL), consisting of two variants: REAL-Prompt and REAL-Linear. First, instead of using the original class names defined by a downstream task, REAL-Prompt adopts the corresponding most frequent synonyms found in the pretraining texts. This simple change already outperforms human-engineered and LLM-generated prompts across nine standard benchmarks. Second, REAL-Linear uses all the synonyms to retrieve a small class-balanced set of data from the pretraining dataset and trains a robust linear classifier atop the VLM. This approach outperforms the recent retrieval-augmented solution REACT, using 400 \times less storage and 10,000 \times less training time. Finally, we show that contemporary text-to-image generators (e.g., DALL-E 3 and SD-XL) may fail to generate images featuring rare concepts. As such, we apply REAL-Prompt to these generators and show that using most frequent synonyms of a rare concept can help them synthesize more accurate images.

Acknowledgements

We thank Tiffany Ling for helping polish figures.

References

[1] Sandhini Agarwal, Gretchen Krueger, Jack Clark, Alec Radford, Jong Wook Kim, and Miles Brundage. Evaluating clip: towards characterization of broader capabilities and downstream implications. *arXiv:2108.02818*, 2021. 2

[2] Stability AI. Stable diffusion online, 2023. 1, 2, 7, 14, 17, 18, 19, 20

[3] James Betker, Gabriel Goh, Li Jing, Tim Brooks, Jianfeng Wang, Linjie Li, Long Ouyang, Joyce Zhuang, Jun-tang andLee, Yufei Guo, Wesam Manassra, Prafulla Dhariwal, Casey Chu, Yunxin Jiang, and Aditya Ramesh. Improving image generation with better captions. *Note on Dalle-3*, 2023. 1

[4] Abeba Birhane, Vinay Uday Prabhu, and Emmanuel Kahembwe. Multimodal datasets: misogyny, pornography, and malignant stereotypes. *arXiv:2110.01963*, 2021. 2

[5] Lukas Bossard, Matthieu Guillaumin, and Luc Van Gool. Food-101—mining discriminative components with random forests. In *Computer Vision—ECCV 2014: 13th European Conference, Zurich, Switzerland, September 6–12, 2014, Proceedings, Part VI 13*, pages 446–461. Springer, 2014. 6, 11

[6] Mehdi Cherti, Romain Beaumont, Ross Wightman, Mitchell Wortsman, Gabriel Ilharco, Cade Gordon, Christoph Schuhmann, Ludwig Schmidt, and Jenia Jitsev. Reproducible scaling laws for contrastive language-image learning. In *CVPR*, 2023. 6

[7] Ching-Yao Chuang, Jampani Varun, Yuanzhen Li, Antonio Torralba, and Stefanie Jegelka. Debiasing vision-language models via biased prompts. *arXiv preprint 2302.00070*, 2023. 2

[8] Mircea Cimpoi, Subhransu Maji, Iasonas Kokkinos, Sammy Mohamed, and Andrea Vedaldi. Describing textures in the wild. In *Proceedings of the IEEE conference on computer vision and pattern recognition*, pages 3606–3613, 2014. 6, 11

[9] Jia Deng, Wei Dong, Richard Socher, Li-Jia Li, Kai Li, and Li Fei-Fei. Imagenet: A large-scale hierarchical image database. In *CVPR*, 2009. 1, 2, 4, 6, 11, 17, 18

[10] Kelvin Guu, Kenton Lee, Zora Tung, Panupong Pasupat, and Mingwei Chang. Retrieval augmented language model pre-training. In *International conference on machine learning*, pages 3929–3938. PMLR, 2020. 2, 3

[11] Patrick Helber, Benjamin Bischke, Andreas Dengel, and Damian Borth. Eurosat: A novel dataset and deep learning benchmark for land use and land cover classification. *IEEE Journal of Selected Topics in Applied Earth Observations and Remote Sensing*, 12(7):2217–2226, 2019. 6, 11, 13

[12] Dan Hendrycks, Steven Basart, Norman Mu, Saurav Kadavath, Frank Wang, Evan Dorundo, Rahul Desai, Tyler Zhu, Samyak Parajuli, Mike Guo, et al. The many faces of robustness: A critical analysis of out-of-distribution generalization. In *Proceedings of the IEEE/CVF International Conference on Computer Vision*, pages 8340–8349, 2021. 6, 8, 11

[13] Dan Hendrycks, Kevin Zhao, Steven Basart, Jacob Steinhardt, and Dawn Song. Natural adversarial examples. In *Proceedings of the IEEE/CVF Conference on Computer Vision and Pattern Recognition*, pages 15262–15271, 2021. 6, 8, 11

[14] Gabriel Ilharco, Mitchell Wortsman, Ross Wightman, Cade Gordon, Nicholas Carlini, Rohan Taori, Achal Dave, Vaishaal Shankar, Hongseok Namkoong, John Miller, Hannaneh Hajishirzi, Ali Farhadi, and Ludwig Schmidt. Openclip, 2021. If you use this software, please cite it as below. 1, 2, 3, 6

[15] Simon Kornblith, Jonathon Shlens, and Quoc V Le. Do better imagenet models transfer better? In *Proceedings of the IEEE/CVF conference on computer vision and pattern recognition*, pages 2661–2671, 2019. 6, 8, 11

[16] Jonathan Krause, Michael Stark, Jia Deng, and Li Fei-Fei. 3d object representations for fine-grained categorization, 2013. 6, 11, 13

[17] Patrick Lewis, Ethan Perez, Aleksandra Piktus, Fabio Petroni, Vladimir Karpukhin, Naman Goyal, Heinrich Kütterl, Mike Lewis, Wen-tau Yih, Tim Rocktäschel, et al. Retrieval-augmented generation for knowledge-intensive nlp tasks. *Advances in Neural Information Processing Systems*, 33:9459–9474, 2020. 2, 3

[18] Alexander Li, Ellis Brown, Alexei A Efros, and Deepak Pathak. Internet explorer: Targeted representation learning on the open web. In *ICML*, 2023. 2, 3

[19] Chunyuan Li, Haotian Liu, Liunian Harold Li, Pengchuan Zhang, Jyoti Aneja, Jianwei Yang, Ping Jin, Houdong Hu, Zicheng Liu, Yong Jae Lee, and Jianfeng Gao. Elevate: A benchmark and toolkit for evaluating language-augmented visual models. *Neural Information Processing Systems*, 2022. 4

[20] Zhiqiu Lin, Samuel Yu, Zhiyi Kuang, Deepak Pathak, and Deva Ramanan. Multimodality helps unimodality: Cross-modal few-shot learning with multimodal models. In *Proceedings of the IEEE/CVF Conference on Computer Vision and Pattern Recognition*, pages 19325–19337, 2023. 2, 5, 7, 11, 13, 15

[21] Haotian Liu, Chunyuan Li, Qingyang Wu, and Yong Jae Lee. Visual instruction tuning. In *NeurIPS*, 2023. 1, 2, 13, 17, 18

[22] Haotian Liu, Kilho Son, Jianwei Yang, Ce Liu, Jianfeng Gao, Yong Jae Lee, and Chunyuan Li. Learning customized visual models with retrieval-augmented knowledge. In *CVPR*, 2023. 2, 3, 6, 7, 8, 13

[23] Shihong Liu, Zhiqiu Lin, Samuel Yu, Ryan Lee, Tiffany Ling, Deepak Pathak, and Deva Ramanan. Language models as black-box optimizers for vision-language models. *arXiv preprint arXiv:2309.05950*, 2023. 3

[24] Subhransu Maji, Esa Rahtu, Juho Kannala, Matthew Blaschko, and Andrea Vedaldi. Fine-grained visual classification of aircraft. *arXiv:1306.5151*, 2013. 6, 11, 17, 18

[25] Ninareh Mehrabi, Fred Morstatter, Nripsuta Saxena, Kristina Lerman, and Aram Galstyan. A survey on bias and fairness in machine learning. *ACM computing surveys (CSUR)*, 54(6):1–35, 2021. 2

[26] Sachit Menon and Carl Vondrick. Visual classification via description from large language models. *arXiv:2210.07183*, 2022. 2, 3, 5, 6, 7, 8, 13, 16

[27] Sachit Menon, Ishaan Preetam Chandratreya, and Carl Vondrick. Task bias in vision-language models. *arXiv:2212.04412*, 2022. 2

[28] Maria-Elena Nilsback and Andrew Zisserman. Automated flower classification over a large number of classes. In *2008 Sixth Indian conference on computer vision, graphics & image processing*, pages 722–729. IEEE, 2008. 4, 6, 11, 17, 18

[29] OpenAI. Gpt-4 technical report, 2023. 1, 2, 3, 4, 5

[30] Shubham Parashar, Zhiqiu Lin, Yanan Li, and Shu Kong. Prompting scientific names for zero-shot species recognition. In *EMNLP*, 2023. 3

[31] Omkar M Parkhi, Andrea Vedaldi, Andrew Zisserman, and CV Jawahar. Cats and dogs. In *2012 IEEE conference on computer vision and pattern recognition*, pages 3498–3505. IEEE, 2012. 4, 6, 11

[32] Sarah Pratt, Ian Covert, Rosanne Liu, and Ali Farhadi. What does a platypus look like? generating customized prompts for zero-shot image classification. In *Proceedings of the IEEE/CVF International Conference on Computer Vision*, pages 15691–15701, 2023. 2, 3, 5, 6, 7, 8, 13, 16

[33] Alec Radford, Jong Wook Kim, Chris Hallacy, Aditya Ramesh, Gabriel Goh, Sandhini Agarwal, Girish Sastry, Amanda Askell, Pamela Mishkin, Jack Clark, et al. Learning transferable visual models from natural language supervision. In *ICML*, 2021. 1, 2, 3, 4, 5, 6, 8, 11, 12, 13, 15, 16

[34] Aditya Ramesh, Mikhail Pavlov, Gabriel Goh, Scott Gray, Chelsea Voss, Alec Radford, Mark Chen, and Ilya Sutskever. Zero-shot text-to-image generation. In *International Conference on Machine Learning*, pages 8821–8831. PMLR, 2021. 1

[35] Christoph Schuhmann, Richard Vencu, Romain Beaumont, Robert Kaczmarczyk, Clayton Mullis, Aarush Katta, Theo Coombes, Jenia Jitsev, and Aran Komatsuzaki. Laion-400m: Open dataset of clip-filtered 400 million image-text pairs. *arXiv:2111.02114*, 2021. 1, 3, 6, 12, 13

[36] Christoph Schuhmann, Romain Beaumont, Richard Vencu, Cade Gordon, Ross Wightman, Mehdi Cherti, Theo Coombes, Aarush Katta, Clayton Mullis, Mitchell Wortsman, et al. Laion-5b: An open large-scale dataset for training next generation image-text models. *Advances in Neural Information Processing Systems*, 35:25278–25294, 2022. 1, 3, 6, 12, 14

[37] Jie-Jing Shao, Jiang-Xin Shi, Xiao-Wen Yang, Lan-Zhe Guo, and Yu-Feng Li. Investigating the limitation of clip models: The worst-performing categories. *arXiv:2310.03324*, 2023. 2

[38] Sheng Shen, Chunyuan Li, Xiaowei Hu, Yujia Xie, Jianwei Yang, Pengchuan Zhang, Zhe Gan, Lijuan Wang, Lu Yuan, Ce Liu, et al. K-lite: Learning transferable visual models with external knowledge. *Advances in Neural Information Processing Systems*, 35:15558–15573, 2022. 3

[39] Zhan Shi, Xu Zhou, Xipeng Qiu, and Xiaodan Zhu. Improving image captioning with better use of captions. *arXiv:2006.11807*, 2020. 1, 2, 4, 7, 14, 17, 18, 19, 20

[40] Hugo Touvron, Louis Martin, Kevin Stone, Peter Albert, Amjad Almahairi, Yasmine Babaei, Nikolay Bashlykov, Soumya Batra, Prajjwal Bhargava, Shruti Bhosale, et al. Llama 2: Open foundation and fine-tuned chat models. *arXiv:2307.09288*, 2023. 4

[41] Catherine Wah, Steve Branson, Peter Welinder, Pietro Perona, and Serge Belongie. The caltech-ucsd birds-200-2011 dataset, 2011. 6, 11

[42] Matthew Wallingford, Vivek Ramanujan, Alex Fang, Aditya Kusupati, Roozbeh Mottaghi, Aniruddha Kembhavi, Ludwig Schmidt, and Ali Farhadi. Neural priming for sample-efficient adaptation. *arXiv:2306.10191*, 2023. 2, 3, 13, 14

[43] Angelina Wang, Alexander Liu, Ryan Zhang, Anat Kleiman, Leslie Kim, Dora Zhao, Iroha Shirai, Arvind Narayanan, and Olga Russakovsky. Revise: A tool for measuring and mitigating bias in visual datasets. *International Journal of Computer Vision*, 130(7):1790–1810, 2022. 2

[44] Haohan Wang, Songwei Ge, Zachary Lipton, and Eric P Xing. Learning robust global representations by penalizing local predictive power. *Advances in Neural Information Processing Systems*, 32, 2019. 6, 8, 11

[45] Xudong Wang, Zhirong Wu, Long Lian, and Stella X Yu. Debiased learning from naturally imbalanced pseudo-labels. In *CVPR*, 2022. 2

[46] Mitchell Wortsman, Gabriel Ilharco, Jong Wook Kim, Mike Li, Simon Kornblith, Rebecca Roelofs, Raphael Gontijo Lopes, Hannaneh Hajishirzi, Ali Farhadi, Hongseok Namkoong, et al. Robust fine-tuning of zero-shot models. In *Proceedings of the IEEE/CVF Conference on Computer Vision and Pattern Recognition*, pages 7959–7971, 2022. 7, 11, 15

[47] Hu Xu, Saining Xie, Xiaoqing Ellen Tan, Po-Yao Huang, Russell Howes, Vasu Sharma, Shang-Wen Li, Gargi Ghosh, Luke Zettlemoyer, and Christoph Feichtenhofer. Demystifying clip data. *arXiv:2309.16671*, 2023. 1, 4, 5

[48] Zhengyuan Yang, Linjie Li, Kevin Lin, Jianfeng Wang, Chung-Ching Lin, Zicheng Liu, and Lijuan Wang. The dawn of lmms: Preliminary explorations with gpt-4v (ision). *arXiv preprint arXiv:2309.17421*, 9, 2023. 1, 2, 13, 17, 18

[49] Kaiyang Zhou, Jingkang Yang, Chen Change Loy, and Ziwei Liu. Learning to prompt for vision-language models. *International Journal of Computer Vision*, 130(9):2337–2348, 2022. 3

[50] Beier Zhu, Kaihua Tang, Qianru Sun, and Hanwang Zhang. Generalized logit adjustment: Calibrating fine-tuned models by removing label bias in foundation models. In *NeurIPS*, 2023. 2

The Neglected Tails of Vision-Language Models

Supplementary Material

Outline

This document supplements the main paper with comprehensive analyses and ablations. Below outlines the document.

- **Section A.** We provide details of the nine benchmark datasets and the four ImageNet variants.
- **Section B.** We report our estimated concept frequency on the other eight benchmark datasets.
- **Section C.** We report REAL performance on head and tail classes across nine benchmark datasets.
- **Section D.** We attach all implementation details of REAL for reproducibility.
- **Section E.** We present further ablations of REAL-Linear to highlight the importance of synonym-based retrieval and cross-modal adaptation.
- **Section F.** We show that the performance gain of REAL can generalize across different architectures, pretraining datasets, and prompt templates.
- **Section G.** We show more failures of state-of-the-art multimodal systems (visual chatbots and text-to-image generative models) on diverse tailed concepts.
- **Section H.** We qualitatively show that REAL-Prompt can help generate images featuring rare concepts.

A. Dataset Details

Table 6 shows the details of the nine benchmarks, including the number of classes and the size of testset. These datasets are widely used in the research community of zero-shot recognition.

Table 6. Details of thirteen benchmark datasets.

Dataset	#Classes	#Testing data	Remark
Flowers [28]	102	2,463	flower classification
Cars [16]	196	8,041	car (brand and year) classification
Aircraft [24]	100	3,333	aircraft classification
Pets [31]	37	3,669	domestic pet classification
Food [5]	101	30,300	food classification
DTD [8]	47	1,692	texture classification
EuroSAT [11]	10	8,100	satellite imagery classification
CUB [41]	200	5,794	bird classification
ImageNet [9]	1,000	50,000	wordnet categories classification
ImageNet-V2 [15]	1,000	30,000	an ImageNet variant of temporal shift
ImageNet-A [13]	200	7,500	an ImageNet variant of adversarial samples
ImageNet-R [12]	200	30,000	an ImageNet variant of artistic renditions
ImageNet-S [44]	1,000	50,000	an ImageNet variant of sketches



(a) dotted vs. polka dotted (b) smeared vs. stained

Figure 6. **Classes in the DTD [8] dataset can be semantically ambiguous.** The texture class dotted is a super-set of another class polka dotted. For another case, people use the class name smeared and stained interchangeably.

B. Results of Concept Frequency Estimation

In Table 7, we plot the concept frequency calculated using our proposed method for the other eight benchmark datasets. Surprisingly, we find that all of them follow an imbalanced distribution (as measured in LAION). Moreover, we plot the per-class zero-shot accuracies grouped by concept frequency and confirm a strong correlation between concept frequency and zero-shot accuracy in the majority of the datasets except for the DTD dataset. For DTD, we find that certain classes can overlap with others. For example, the dotted and polka dotted, smeared and stained (see Figure 6). Such ambiguous labeling makes DTD an outlier for our frequency analysis.

C. Performance Breakdown of REAL

In Table 8, we show the improvement of REAL on the head and tail classes across nine benchmark datasets. We emphasize that REAL can significantly lift both head and tail accuracy on downstream tasks using the original pre-training data.

D. Further Details for REAL

Synonym filtering in REAL-Prompt. We use Open-CLIP’s text encoder to filter out ChatGPT-generated synonyms that might be confused with other downstream concepts. Specifically, we retain only those synonyms that have the highest cosine similarity scores with their original class names (not with another downstream concept). This filtering step is critical to REAL-Prompt’s performance as shown in Table 15.

Linear probing in REAL-Linear. We follow previous work [20, 46] and adopt the same procedure and hyperparameters to learn a robust cross-modal classifier. Specifically, we initialize the weights of the cross-modal linear classifier using averaged text features constructed using the most frequent synonyms and OpenAI templates [33]. Next,

Table 7. **Vision-language models (VLMs) inherit long tails from their pretraining data.** We show that concepts from the other eight benchmark datasets all follow a long-tailed distribution in the pretraining datasets (e.g. LAION-400M [35], LAION-2B [36]). The strong correlation between concept frequency and accuracy prevalently exists among the datasets. For DTD, the trend deteriorates because of the ambiguous labeling of class names (see Figure 6).

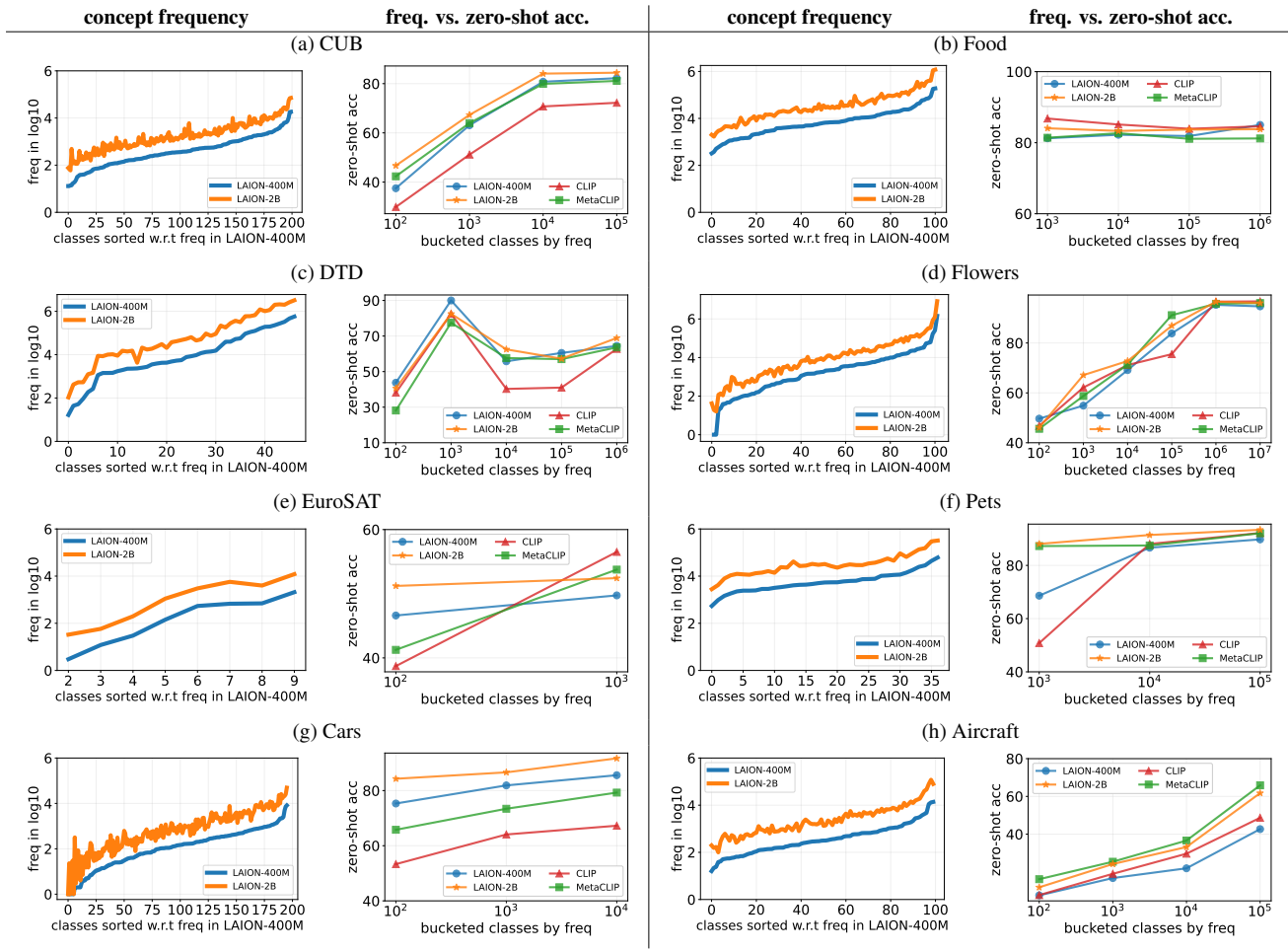


Table 8. **Breakdown improvements of REAL.** REAL-Prompt and REAL-Linear (500 retrieved examples per concept) can significantly improve upon the baseline performance using the OpenAI templates [33] on nine standard zero-shot recognition benchmark datasets. We define the tail as the 20% least frequent classes and the rest as the head for each dataset. REAL significantly lifts both head and tail accuracies on these datasets.

Method	ImageNet		Flowers		Cars		Aircraft		CUB		Pets		Food		DTD		EuroSAT		Avg		
	Head	Tail	Head	Tail	Head	Tail	Head	Tail	Head	Tail	Head	Tail	Head	Tail	Head	Tail	Head	Tail	Head	Tail	
LAION 400M	OpenAI templates	64.8	55.2	70.0	50.6	81.1	72.9	18.9	8.4	69.1	40.1	87.4	83.5	80.4	82.5	54.3	55.2	65.0	23.9	65.7	52.5
	REAL-Prompt	65.4	56.2	76.8	58.8	85.2	73.7	20.8	7.3	69.3	40.6	88.7	88.6	80.5	82.3	59.3	62.0	64.3	41.9	67.8	56.8
	+0.6	+1.0	+6.8	+8.2	+4.1	+0.8	+1.9	-1.1	+0.2	+0.5	+1.3	+5.1	+0.1	-0.2	+5.0	+6.8	-0.7	+18.0	+2.1	+4.3	
	REAL-Linear (500)	67.8	58.9	82.4	57.2	87.0	73.2	34.4	10.0	79.3	50.4	89.7	87.7	80.8	83.6	60.8	63.5	69.9	19.2	72.5	56.0
LAION 2B	OpenAI templates	68.0	61.0	75.6	50.5	87.0	82.5	27.9	11.5	73.0	49.0	90.5	90.6	82.0	85.1	58.0	55.2	54.0	38.1	68.6	58.4
	REAL-Prompt	68.2	61.6	79.4	55.1	89.2	80.8	29.3	11.3	72.8	47.7	91.5	92.8	82.1	85.1	64.4	63.5	51.6	58.7	69.8	61.8
	+0.2	+0.6	+3.8	+4.6	+2.2	-1.7	+1.4	-0.2	-0.2	-1.3	+1.5	+2.2	+0.1	+0.0	+6.4	+8.3	-2.4	+20.6	+1.2	+3.4	
	REAL-Linear (500)	69.8	64.8	84.1	66.9	90.0	82.3	45.4	25.5	82.4	62.2	91.5	92.6	82.3	86.2	64.5	70.0	76.0	22.0	76.2	63.6
	+1.8	+3.8	+8.5	+16.4	+3.0	-0.2	+17.6	+14.0	+9.4	+13.2	+1.0	+2.0	+0.3	+1.1	+6.5	+14.8	+22.0	-16.1	+7.6	+5.2	

we stick to the reported [20] learning rate of 1e-4 with a cosine annealing schedule, weight decay of 1e-2, batch size of 32, and training epochs of 10. Finally, we average the learned cross-modal classifier weights with the zero-shot classifier weights (as shown in Figure 4). We apply the same set of hyperparameters for all datasets and model architectures. We will release our code and retrieved data for reproducibility.

E. More Ablations of REAL-Linear

In this section, we show that synonym-based retrieval and cross-modal adaptation are crucial for the performance of REAL-Linear. We also explain the lower performance of REAL-Linear on Stanford Cars dataset. Lastly, we ablate the retrieval sizes v.s. zero-shot accuracies.

Synonyms help retrieve diverse data. It is crucial to retrieve images whose captions contain any of the concept synonyms instead of just the name predefined by the downstream task. Table 9 shows that using all synonyms can retrieve more diverse images for a performance boost of 4% from 64.2% to 68.2% when averaged across eight benchmark datasets, surpassing REACT Locked-Text’s 65.5%. In addition, Table 10 shows that REAL-Linear outperforms another retrieval-augmented method Neural Priming [42], which does not consider concept synonyms for retrieval. For a fair comparison, we follow [42] to use 100 retrieved images per class because they do not release the models and hyperparameters.

Learning robust cross-modal classifiers. We show that cross-modal adaptation [20], which uses both text and image features to learn a linear classifier, is more robust against the distribution shifts between retrieved (pretraining) data and target domains. Concretely, Table 11 shows that performing naive linear probing using only retrieved images achieves lower accuracy by 6.4% averaged across all benchmark datasets, sometimes underperforms the zero-shot classifier [33] constructed using OpenAI prompt templates [33]. This shows that using both images and texts can effectively reduce overfitting to retrieved pretraining data.

Remarks on REAL-Linear’s performance on the Stanford Cars dataset. Table 1 shows that the performance of our REAL-Linear on the Cars dataset [16] is 4% lower than that of REACT [22], despite that we relax the string matching criteria (by matching partial names) to retrieve more relevant images. We attribute the performance gap to the limited images retrieved from LAION-400M [35], owing to the fine-grained nature of the class names, e.g. “Audi S6 Sedan 2011”. Supporting evidence is shown in Table 9, where using synonyms for retrieval increases the accuracy of Cars from 71.1% to 84.4%. This suggests future work on better retrieval methods for datasets with specific brand names.



Figure 7. **Large distribution shifts between LAION and EuroSAT.** We compare two randomly sampled satellite images from LAION and EuroSAT, for the class Herbaceous Vegetation and Sea Lake, respectively. Images from LAION present higher resolution and more distinct features while the EuroSAT images are blurry and lack informative features.

Remarks on retrieval sizes. Retrieving more pretraining examples generally helps REAL-Linear achieve higher accuracies for zero-shot recognition, as shown in Table 12. Yet, increasing the retrieval size from 100 to 500 per concept only improves accuracy by 0.9% (averaged over nine benchmarks). As such, we adopt 500 for our major experiments in this paper.

F. Generalization Performance of REAL

In this section, we show that REAL generalizes across model architectures, datasets, and prompt templates.

Generalizing across architectures and datasets. Table 13 shows that REAL-Linear consistently improves the zero-shot performance of OpenCLIP across different ViT architectures (B/32, B/16, and L/14) and LAION datasets (400M and 2B). Yet, both REAL-Linear and REACT [22] fail to improve on the EuroSAT dataset [11], presumably because satellite imagery is very rare in LAION (e.g., we can retrieve at most one image for Annual Crop and Herbaceous Vegetation). In addition, the few retrieved satellite images in LAION are drastically different from EuroSAT testset images due to sensor shifts, as shown in Figure 7.

Generalizing across prompt templates. Table 14 shows that REAL-Prompt is effective regardless of the prompt templates (OpenAI [33], DCLIP [26], and CuPL [32]).

G. More Failures of Multimodal Systems

In Figure 8 and 9, we show more failure cases of state-of-the-art multimodal systems on tailed concepts identified by our frequency estimation method. These tailed concepts are randomly sampled from nine benchmark datasets and span across a variety of domains, including birds, flowers, fungi, snakes, frogs, fish, household items, and more. We qualitatively test the visual recognition abilities of two most popular visual chatbots: GPT4-V [48] (trained on proprietary data) and LLaVA1.5 [21] (trained on open-source data using a frozen CLIP image encoder). We also test the image generation abilities of two most popular generative models:

Table 9. **Using concept synonyms helps retrieve more diverse pretraining images.** Retrieving images whose captions contain any of the concept synonyms (instead of just the name predefined by the downstream task) can improve the performance of REAL-Linear (using 500 images per class). We attach the performance of REACT Locked-Text (using 10K images per class) for reference.

Method	Images per class	ImageNet	Flowers	Cars	Aircraft	Pets	Food	DTD	EuroSAT	Avg
REACT Locked-Text	10K	65.7	73.1	88.5	24.5	89.2	81.8	49.8	51.1	65.5
REAL-Linear (without synonyms)	500	64.6	72.6	71.1	27.9	88.6	81.9	56.3	50.8	64.2
REAL-Linear (with synonyms)	500	65.9	78.8	84.4	29.6	89.5	81.4	61.5	51.5	67.8

Table 10. **REAL-Linear outperforms Neural Priming.** We compare REAL-Linear with Neural Priming [42] using the ViT-B/16 model pre-trained on LAION-2B [36]. REAL-Linear consistently outperforms Neural Priming on all their reported benchmarks, presumably because Neural Priming does not consider synonyms for retrieval.

Method	Images per class	ImageNet	Cars	Flowers	Aircraft	Food	Pets	Avg
Neural Priming	100	70.8	89.3	79.8	33.0	86.7	91.9	75.3
REAL-Linear	100	71.9	90.3	81.9	38.7	86.7	92.2	77.0

DALL-E 3 [39] (trained on proprietary data) and Stable Diffusion XL [2] (trained on open-source data using a frozen CLIP text encoder). We observe that these systems fail to recognize or generate more than half of the tailed concepts we sampled. In particular, LLaVA1.5 and Stable Diffusion XL fail on all these tailed concepts, suggesting a large performance gap between proprietary and open-source multi-modal systems.

H. REAL-Prompt for Generative Models

Figure 10 and 11 contains qualitative results of REAL-Prompt on state-of-the-art text-to-image generative models including DALL-E 3 [39] and Stable Diffusion XL [2]. This shows that using most frequent synonyms can help generate correct images for tailed concepts. We also note that our method is more effective on the more capable generative model DALL-E 3, presumably because it is trained with more data than open-source Stable Diffusion XL. This suggests opportunities for future work to improve open-source VLMs on image synthesis for rare concepts.

Table 11. **Cross-modal adaptation improves the robustness of REAL-Linear.** We highlight that using both images and texts during training can help address the distribution shifts between pretraining data and target domains. Concretely, we adopt cross-modal WiSE-FT [20, 46], which first learns a cross-modal linear classifier using both retrieved image features and text features constructed using the most frequent concept synonyms and OpenAI templates [33]. This cross-modal classifier is then ensembled with a zero-shot classifier whose weights are text features of the most frequent synonyms averaged across OpenAI prompt templates. We show that this cross-modal strategy is much more robust against vanilla image-only linear probing that uses only retrieved image features, which overfits to retrieved data and sometimes underperforms the zero-shot classifier.

Method	ImageNet	Flowers	Cars	Aircraft	CUB	Pets	Food	DTD	EuroSAT	Avg
OpenAI templates [33]	62.9	68.0	79.2	16.7	63.8	86.7	80.9	54.5	51.5	62.7
REAL-Linear (image-only)	62.1 ^{-0.8}	78.0 ^{+10.0}	77.5 ^{-1.7}	33.1 ^{+16.4}	73.1 ^{+9.3}	86.1 ^{-0.6}	79.5 ^{-1.4}	53.8 ^{-0.7}	15.6 ^{-35.9}	62.4 ^{-0.3}
REAL-Linear (cross-modal)	65.9 ^{+3.0}	78.8 ^{+10.8}	84.1 ^{+7.9}	29.6 ^{+12.9}	74.0 ^{+10.2}	89.5 ^{+2.8}	81.4 ^{+0.5}	61.5 ^{+6.2}	51.5 ^{+0.0}	67.8 ^{+6.1}

Table 12. **Zero-shot accuracy vs. retrieval size.** We conducted an ablation study the impact of retrieval size for REAL-Linear, and for comparison, we included results using OpenAI templates and our REAL-Prompt. Notably, even with a smaller retrieval size of 100 images per concept, we achieve strong performance (only 1% lower on avg.), though our best results come with a retrieval size of 500 images per concept.

Number of shots	ImageNet	Flowers	Cars	Aircraft	CUB	Pets	Food	DTD	EuroSAT	Avg
OpenAI templates [33]	62.9	68.0	79.2	16.7	63.8	86.7	80.9	54.5	51.5	62.7
REAL-Prompt	63.6	76.6	82.7	18.0	64.0	88.8	81.0	59.9	57.5	65.8 ^{+3.1}
REAL-Linear (100)	65.3	77.8	84.0	25.1	72.4	89.3	81.0	60.4	53.3	67.6 ^{+4.9}
REAL-Linear (500)	65.9	78.8	84.4	29.6	74.0	89.5	81.4	61.5	51.5	68.5 ^{+5.8}

Table 13. **REAL-Linear generalizes across different pretraining datasets and architectures.** REAL-Linear consistently achieves performance gains with three OpenCLIP architectures (ViT B/32, B/16, and L/14) and pretraining datasets (LAION 400M and 2B). For reference, we attach the performance REACT reported on these benchmarks. Notably, our REAL-Linear (500 examples per class) even outperforms REACT Gated-Image (10K examples per class) when both use a larger visual encoder ViT-L/14. We highlight the **best accuracy** in bold and underline the second best numbers for ImageNet.

Arch	Method	ImageNet	Flowers	Cars	Aircraft	CUB	Pets	Food	DTD	EuroSAT	Avg
ViT	OpenAI templates [33]	62.9	68.0	79.2	16.7	63.8	86.7	80.9	56.1	51.5	62.6
	REACT Locked-Text (10K)	<u>65.7</u>	73.1	88.5	24.5	—	89.2	81.8	49.8	51.1	—
	REACT Gated-Image (10K)	64.2	72.3	88.1	24.8	—	89.5	83.0	51.4	45.4	—
	REAL-Linear (500)	65.9	78.8	84.1	29.6	74.0	89.5	81.4	61.5	51.5	68.5
LAION 400M	OpenAI templates [33]	67.0	69.2	83.6	17.7	67.2	89.3	86.2	51.3	50.3	64.6
	ViT	REACT Locked-Text (10K)	69.9	—	—	—	—	—	—	—	—
	B/16	REACT Gated-Image (10K)	70.5	—	—	—	—	—	—	—	—
	REAL-Linear (500)	<u>69.6</u>	80.6	86.5	31.5	79.1	91.3	86.4	61.4	51.9	71.0
ViT	OpenAI templates [33]	<u>72.7</u>	75.4	89.5	24.9	76.4	91.8	90.0	60.2	62.3	71.5
	REAL-Linear (500)	74.4	85.4	91.0	40.2	84.8	93.4	90.3	66.5	59.8	76.2
B/32	OpenAI templates [33]	66.6	71.8	86.0	24.5	68.5	90.6	82.7	56.1	48.0	66.1
	ViT	REACT Locked-Text (10K)	67.5	—	—	—	—	—	—	—	—
	REACT Gated-Image (10K)	69.6	—	—	—	—	—	—	—	—	—
	REAL-Linear (500)	<u>68.8</u>	80.6	88.4	41.3	78.5	91.7	83.1	65.6	51.9	72.2
LAION 2B	ViT	OpenAI templates [33]	<u>70.2</u>	71.4	88.2	26.9	72.7	90.5	86.5	56.3	53.4
	B/16	REAL-Linear (500)	72.4	83.4	90.3	45.6	83.6	92.2	87.1	66.0	46.9
	ViT	OpenAI templates [33]	75.3	75.2	91.9	36.6	78.5	93.2	91.0	62.8	64.6
	REAL-Linear (500)	76.9	86.5	92.6	55.3	87.5	94.7	91.2	69.4	57.9	79.1

Table 14. **REAL-Prompt generalizes across prompt templates.** We show that REAL-Prompt (using the most frequent synonyms) can improve upon both OpenAI prompt templates [33] and LLM-generated templates such as DCLIP [26] and CuPL [32].

Arch	Method	ImageNet	Flowers	Cars	Aircraft	CUB	Pets	Food	DTD
ViT-B/32	OpenAI templates [33]	62.9	68.0	79.2	16.7	63.8	86.7	80.9	54.5
	+ REAL-Prompt	63.6	76.6	82.7	18.0	64.0	88.8	81.0	59.9
	DCLIP [26]	62.1	—	—	—	64.5	84.6	80.1	51.4
	+ REAL-Prompt	62.9	—	—	—	64.7	88.1	80.0	55.5
	CuPL [32]	63.7	65.8	80.0	17.8	—	87.4	79.5	59.1
	+ REAL-Prompt	64.2	72.3	81.7	18.3	—	88.0	79.5	59.3
LAION-400M	OpenAI templates [33]	67.0	69.2	83.6	17.7	67.2	89.3	86.2	51.0
	+ REAL-Prompt	67.6	77.1	84.4	19.5	67.3	91.0	86.3	58.1
	DCLIP [26]	65.8	—	—	—	68.6	86.2	85.2	51.1
	+ REAL-Prompt	66.2	—	—	—	68.6	89.8	85.2	57.1
	CuPL [32]	67.8	67.9	83.4	18.6	—	89.7	85.2	57.9
	+ REAL-Prompt	68.1	73.1	84.0	18.8	—	90.5	85.2	59.8
ViT-L/14	OpenAI templates [33]	72.7	75.4	89.5	24.9	76.4	91.8	90.0	60.2
	+ REAL-Prompt	72.9	82.9	89.9	26.0	76.4	93.3	90.2	63.6
	DCLIP [26]	71.8	—	—	—	77.2	89.2	89.3	57.7
	+ REAL-Prompt	72.3	—	—	—	77.3	92.1	89.4	60.5
	CuPL [32]	73.3	76.9	89.3	27.5	—	92.4	89.4	65.4
	+ REAL-Prompt	73.7	82.4	89.6	28.2	—	92.8	89.4	65.7
ViT-B/32	OpenAI templates [33]	66.6	71.8	86.0	24.5	68.5	91.8	82.7	57.4
	+ REAL-Prompt	66.9	76.2	87.5	25.6	68.2	91.8	82.7	64.2
	DCLIP [26]	65.7	—	—	—	68.5	90.5	81.2	53.2
	+ REAL-Prompt	66.0	—	—	—	68.2	90.6	81.2	57.7
	CuPL [32]	67.0	69.5	86.5	26.5	—	91.0	81.6	62.7
	+ REAL-Prompt	67.3	74.1	87.6	27.4	—	91.1	81.6	63.8
LAION-2B	OpenAI templates [33]	70.2	71.4	88.2	26.9	72.7	91.6	86.5	57.9
	+ REAL-Prompt	70.3	78.6	88.7	28.7	72.6	91.7	86.6	64.8
	DCLIP [26]	69.5	—	—	—	73.6	91.6	86.0	58.1
	+ REAL-Prompt	69.7	—	—	—	73.5	91.7	86.0	62.7
	CuPL [32]	70.6	70.6	88.6	29.6	—	91.1	86.2	63.8
	+ REAL-Prompt	70.8	76.6	89.4	30.0	—	91.1	86.2	64.9
ViT-L/14	OpenAI templates [33]	75.3	75.2	91.9	36.6	78.5	94.1	91.0	64.1
	+ REAL-Prompt	75.4	83.4	92.1	37.6	78.5	94.2	91.0	67.8
	DCLIP [26]	74.5	—	—	—	78.3	93.2	90.8	63.1
	+ REAL-Prompt	74.9	—	—	—	78.2	93.2	90.8	64.4
	CuPL [32]	75.7	75.4	92.6	41.2	—	94.3	90.6	68.7
	+ REAL-Prompt	75.9	82.0	92.1	41.4	—	94.2	90.6	68.8

Table 15. **The importance of synonym-filtering for REAL-Prompt.** After obtaining synonyms from ChatGPT, we use OpenCLIP’s text encoder to filter the synonyms that might be confused with other downstream concepts. We show that this filtering step is critical for REAL-Prompt’s performance.

	ImageNet	Flowers	Cars	Aircraft	CUB	Pets	Food	DTD
REAL-Prompt w/o Synonym Filtering	50.5	45.0	59.3	9.5	55.6	39.9	63.5	10.9
REAL-Prompt w/ Synonym Filtering	63.6	76.6	82.7	18.0	64.0	88.8	81.0	59.9

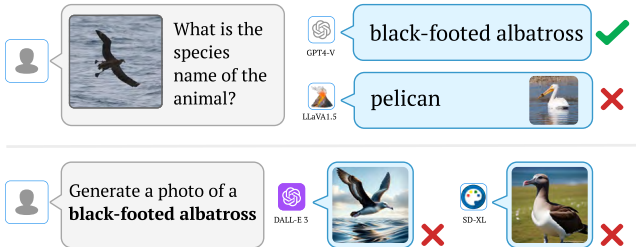
Concept: bank swallow

Definition: a small bird with a brown back and white belly.



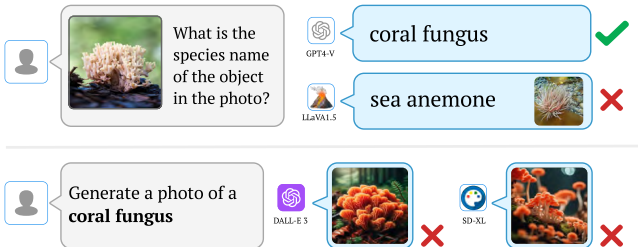
Concept: black-footed albatross

Definition: a large seabird with black or dark feet.



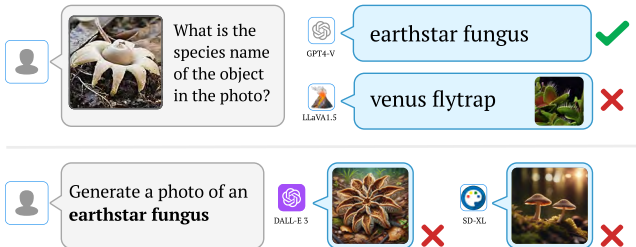
Concept: coral fungus

Definition: a group of mushrooms resembling ocean corals.



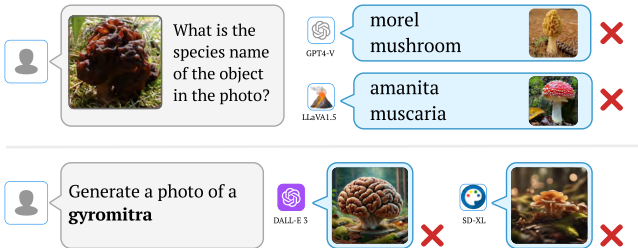
Concept: earthstar fungus

Definition: a fungus with a star-shaped appearance.



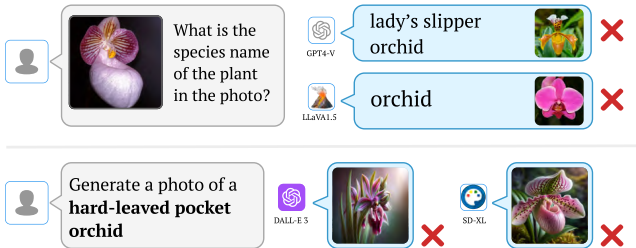
Concept: gyromitra

Definition: a mushroom with brain-like wrinkled cap.



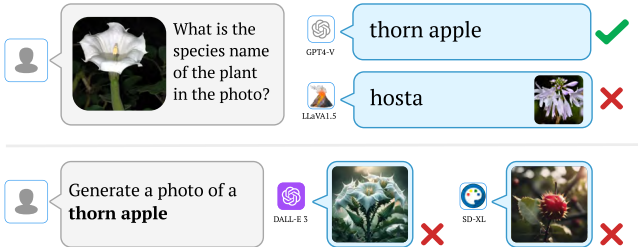
Concept: hard-leaved pocket orchid

Definition: an orchid with a large pouch and symmetrical petals.



Concept: thorn apple

Definition: a flower with large, trumpet-shaped flowers.



Concept: tailed frog

Definition: a primitive frog with a short "tail".



Figure 8. **State-of-the-art multimodal systems fail to recognize or generate tailed concepts (part 1).** We show more failure cases of popular multimodal systems (GPT4-V [48], LLaVA1.5 [21], DALL-E 3 [39], and Stable Diffusion XL [2]) on tailed concepts sampled from standard benchmark datasets such as ImageNet [9], Flowers [28], Aircraft [24], and etc. For GPT4-V and LLaVA1.5, we include example images of incorrectly predicted classes to show that visual chatbots often misclassify rare concepts as some similar-looking yet more common concepts. We include a definition for each tailed concept to show that DALL-E 3 and Stable Diffusion (SD-XL) can fail to capture the correct colors, shapes, and other characteristics of these concepts.

Concept: electric ray

Definition: a fish with rounded body, short thick tails, and caudal fins.



Concept: night snake

Definition: a small light brown or beige colored snake.



Concept: longnose gar

Definition: a gar fish with long snout.



Concept: ring-necked snake

Definition: a small snake with a yellowish ring around the neck.



Concept: sidewinder rattlesnake

Definition: a snake with Horn-like superocular scales on their heads.



Concept: pan flute

Definition: a flute with multiple pipes of gradually increasing length.



Concept: monkey face orchid

Definition: a rare and unusual orchid that resembles a monkey's face.

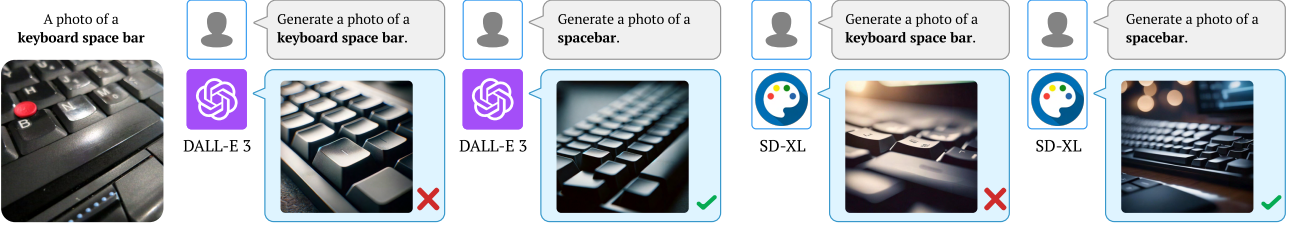


Concept: BAE 146-200

Definition: a passenger plane with four engines.



Figure 9. **State-of-the-art multimodal systems fail to recognize or generate tailed concepts (part 2).** We show more failure cases of popular multimodal systems (GPT4-V [48], LLaVA1.5 [21], DALL-E 3 [39], and Stable Diffusion XL [2]) on tailed concepts sampled from standard benchmark datasets such as ImageNet [9], Flowers [28], Aircraft [24], and etc. For GPT4-V and LLaVA1.5, we include example images of incorrectly predicted classes to show that visual chatbots often misclassify rare concepts as some similar-looking yet more common concepts. We include a definition for each tailed concept to show that DALL-E 3 and Stable Diffusion (SD-XL) can fail to capture the correct colors, shapes, and other characteristics of these concepts.



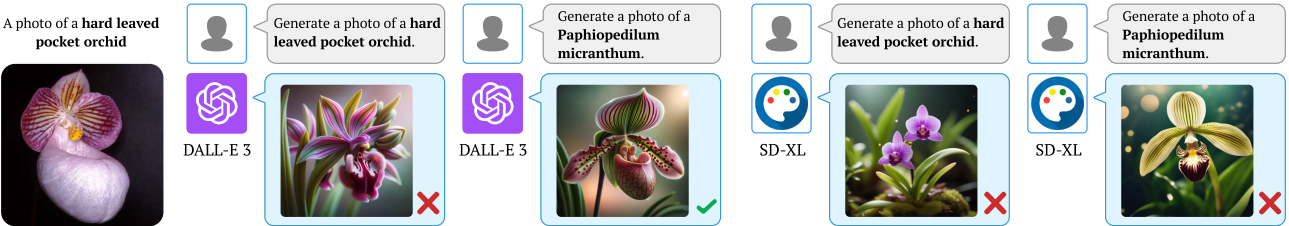
(a) keyboard space bar, a **long bar** at the **bottom** of a computer keyboard. When prompted with the original concept name (keyboard space bar), both DALL-E 3 and SD-XL fail by focusing on generating images of the keyboard. However, when prompted with the most frequent synonyms (space bar), both are able to generate correct images.



(b) BAE 146-200, an airplane with **4 engines**. When prompted with the original concept name (BAE 146-200), both DALL-E 3 and SD-XL fail by generating only 2 engines. However, when prompted with the most frequent synonym (avro rj85), both are able to generate correct images with 4 engines.

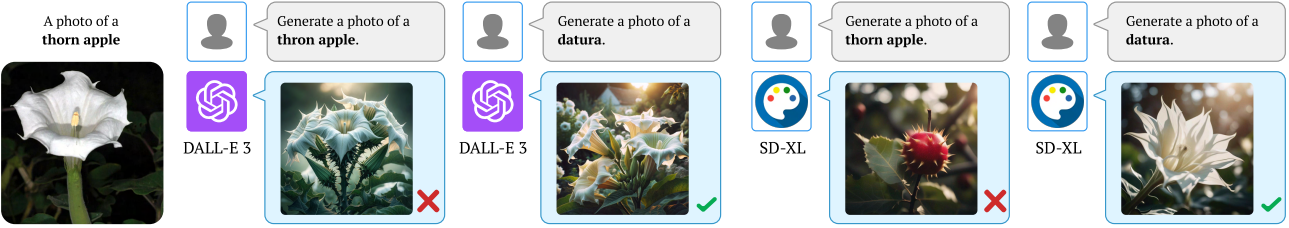


(c) bank swallow, a small bird with **brown back** and **white belly**. When prompted with the original concept name (bank swallow), both DALL-E 3 and SD-XL generate incorrect images of birds with incorrect black backs. However, prompting with the most frequent synonym (sand martin) guides both systems to produce correct images.

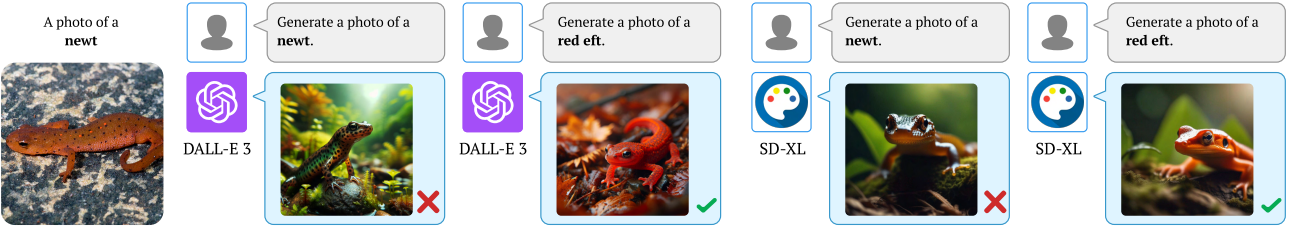


(d) hard leaved pocket orchid, a type of orchid with a **distinctive pouch** and **symmetrical large petals**. When prompted with the original concept name (hard leaved pocket orchid), both DALL-E 3 and SD-XL generate incorrect images (note the missing pocket and shape of the petals). However, when prompted with the most frequent synonym (Paphiopedilum micranthum), DALL-E 3 produces the correct image. In contrast, SD-XL is able to recover the shape of petals but still misses the pocket.

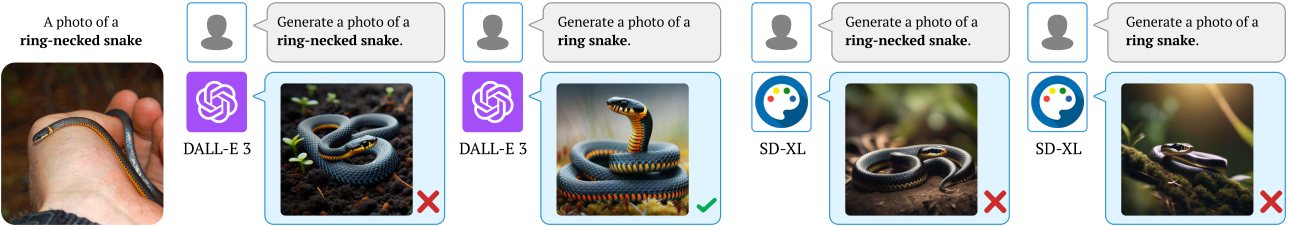
Figure 10. Prompting with the most frequent synonym can help DALL-E 3 and Stable Diffusion generate correct images (part 1). We show more examples when DALL-E 3 [39] and Stable Diffusion XL (SD-XL) [2] initially fail to generate correct images for tailed concepts when prompted with their original concept names in standard classification benchmark datasets. We sample diverse tail concepts covering a variety of domains including household items, birds, flowers, insects, reptiles, and etc. We show that REAL-Prompt (prompting with the most frequent synonyms) often helps DALL-E 3 and Stable Diffusion produce correct images. We notice that for the hard leaved pocket orchid and ring-necked snake, the generated images of SD-XL improve but are still inaccurate. This suggests future work to improve open-source generative models on rare concepts.



(e) thorn apple, a plant with **large, white, trumpet-shaped** flowers. When prompted with the original concept name (thorn apple), DALL-E 3 generates an image with sharp thorns along its stem. Even worse, SD-XL takes the name superficially and generates an apple with thorns. On the contrary, prompting with the most frequent synonym (datura) leads to correct images in both systems.



(f) newt, a type of salamander known for its **bright orange to red color** and **scattered darker spots**. When prompted with the original concept name (newt), both DALL-E 3 and SD-XL fail by generating a green-colored skin. However, prompting with the most frequent synonym (red eft) leads to the correct red-colored body.



(g) ring-necked snake, a small snake with a **yellowish ring around the neck**. When prompted with the original concept name (ring-necked snake), both DALL-E 3 and SD-XL fail by missing the yellow ring around the snake's neck. However, prompting with the most frequent synonym (ring snake) helps DALL-E 3 recover the ring. Meanwhile, SD-XL still fails to capture the ring which is likely due to insufficient relevant images in its pretraining data.

Figure 11. Prompting with the most frequent synonym can help DALL-E 3 and Stable Diffusion (SD-XL) generate correct images (part 2). We show more examples when DALL-E 3 [39] and Stable Diffusion XL (SD-XL) [2] initially fail to generate correct images for tailed concepts when prompted with their original concept names in standard classification benchmark datasets. We sample diverse tail concepts covering a variety of domains including household items, birds, flowers, insects, reptiles, etc. We show that REAL-Prompt (prompting with the most frequent synonyms) often helps DALL-E 3 and Stable Diffusion produce correct images. We notice that for the hard-leaved pocket orchid and ring-necked snake, the generative images of SD-XL improve but are still inaccurate. This suggests future work to improve open-source generative models on rare concepts.